Table 2. *Starting set defined by SIMPEL for PGE2*

| *h* | *k* | *l* | *E* | (symbolic) phase |
|---|---|---|---|---|
| 5 | −9 | 1 | 3·01 | 0 } origin-defining reflections |
| 5 | −10 | 1 | 2·82 | 0 |
| 9 | 0 | 2 | 2·40 | 0 |
| −1 | 2 | 1 | 3·18 | *a* |
| 7 | 1 | 2 | 3·81 | *b* |
| −1 | 1 | 1 | 2·76 | *c* |
| 7 | −4 | 2 | 2·81 | *d* |
| 7 | 4 | 2 | 2·75 | *e* |

were symbolically phased and for 23 reflections more than one symbolic phase was found. 61 quartets with $E4 > 1{\cdot}2$ contributed to ENQUAC. Refinement of the 48 lowest of the 1024 calculated ENQUAC values yielded 18 possible solutions. For the calculation of ENQUIC, 42 quintets with $E5 > 0{\cdot}55$ could be used. Refinement of the 48 lowest minima yielded 17 possible solutions; 12 of them were approximately identical to possible solutions of ENQUAC.

These 12 solutions were refined with the enantiomorph-specific refinement and extension procedure. After the refinement the ten strongest peaks in the *E* map of solution number 6 in order of ENQUAC (solution number 3 in order of ENQUIC, solution number 3 in order of ENQUAC + ENQUIC) revealed eight atoms and two atoms of the enantiomorph. The next 20 strongest peaks revealed seven atoms, seven atoms of the enantiomorph and six spurious peaks.

The *E* map of the best solution in order of the combined ENQUAC–ENQUIC figure of merit was not interpretable.

The authors thank Dr C. Stam for a critical reading of the manuscript.

### References

DeTitta, G. T., Edmonds, J. W., Langs, D. A. & Hauptman, H. (1975). *Acta Cryst.* A**31**, 472–479.
Edmonds, J. W. & Duax, W. L. (1974*a*). *Prostaglandins*, **5**, 275–281.
Edmonds, J. W. & Duax, W. L. (1974*b*). *Am. Cryst. Assoc. Spring Meeting, Univ. Calif.* Abstract *A*5.
Fischer, J., Hancock, J. & Hauptman, H. (1970). Report No. 7132. Naval Research Laboratory, Washington, D.C.
Germain, G., Main, P. & Woolfson, M. M. (1971). *Acta Cryst.* A**27**, 368–376.
Giacovazzo, C. (1975). *Acta Cryst.* A**31**, 252–259.
Giacovazzo, C. (1977). *Acta Cryst.* A**33**, 527–531.
Gilmore, C. (1977). *Acta Cryst.* A**33**, 712–716.
Gilmore, C. (1978). Private communication.
Hauptman, H. (1974). *Acta Cryst.* A**30**, 472–476.
Hauptman, H. (1975). *Acta Cryst.* A**31**, 680–687.
Hauptman, H., Fischer, J., Hancock, H. & Norton, D. A. (1969). *Acta Cryst.* B**25**, 811–814.
Hauptman, H. (1978). Private communication.
Hauptman, H. & Fortier, S. (1977). *Acta Cryst.* A**33**, 575–580.
Kanters, J. A. & van Veen, A. M. (1973). *Cryst. Struct. Commun.* **2**, 261–265.
Karle J. & Hauptman, H. (1958). *Acta Cryst.* **11**, 264–269.
Lessinger, L. (1976). *Acta Cryst.* A**32**, 538–550.
Mairesse, G. & Dracke, M. (1978). *Acta Cryst.* B**34**, 1771–1776.
Overbeek, A. R., van der Putten, N., Olthof, G. J. & Schenk, H. (1977). *SIMPEL* manual, Amsterdam.
Putten, N. van der (1978). In preparation.
Putten, N. van der & Schenk, H. (1976). *K. Ned. Akad. Wet. Proc.* B**79**, 344–352.
Putten, N. van der & Schenk, H. (1977). *Acta Cryst.* A**33**, 856–858.
Schenk, H. (1972) *Acta Cryst.* A**28**, 412–422.
Schenk, H. (1974). *Acta Cryst.* A**30**, 477–481.
Schenk, H. (1975). *Acta Cryst.* A**31**, 259–263.
Schenk, H. (1976). Proc. Buffalo Direct Methods Symp., 1976.
Schenk, H. & Putten, N. van der (1977). *Acta Cryst.* A**33**, 368–372.
Sint, L. & Schenk, H. (1975). *Acta Cryst.* A**31**, S22.
Spek, A. L. (1975). Thesis, Utrecht.

*Acta Cryst.* (1979). A**35**, 387–390

# Electron Microscopy Studies of $Mo_3CoSi$

By Lars Stenberg

*Inorganic Chemistry* 2, *Chemical Center, PO Box* 740, *S*-220 07 *Lund, Sweden*

(*Received* 17 *June* 1978; *accepted* 27 *November* 1978)

## Abstract

Crystals of $Mo_3CoSi$ were studied with a high-resolution electron microscope. Planar defects of different kinds were easily and frequently observed. The structure of one kind of defect can be derived with crystallograpic shear operations.

## Introduction

The principles of formation of the so-called tetrahedrally close-packed alloy structures, involving different crystallographic operations and intergrowth, have recently been described by Andersson (1978). In this way it is possible to describe and predict defects and a

0567-7394/79/030387-04$01.00 

number of new structure-types, using the simple $Cr_3Si$ or $\beta$-tungsten structure type as parent structure.

The lattice image technique of high-resolution electron microscopy has been a powerful tool to explain different kinds of defects in detail, especially in oxide systems. The use of this technique was recently extended to include some of the tetrahedrally close-packed structures of transition elements (Stenberg & Andersson, 1978). It was shown that some of the phases identified contained planar defects of chemical twinning and intergrowth. In order to find other types of defects, studies have now been carried out on $Mo_3CoSi$, a structure determined by Gladyshevskii, Kripyakevich & Skolozdra (1967).

## Experimental

The samples were prepared in sealed silica tubes and heated for seven days at 1273 K. The crystals, which were brittle, were ground in an agate mortar, and transferred to a holey carbon film coated on a copper grid.

The microscope used was a Philips EM400 operating at 120 kV and with an objective aperture of 100 μ, corresponding to 2·2 Å.

The crystals were aligned along the short $c$ axis, 4·89 Å, so the beam was perpendicular to the tetragonal axes (12·85 Å).

## Results

In Fig. 1 the real structure of $Mo_3CoSi$ is projected along the $c$ axis with the tetragonal cell outlined. The shadowed areas indicate the so-called *Tetraedersterns*, with atoms on 0 and $\frac{1}{2}$. Andersson (1978) describes this as a structure built up by 2 × 2 $Cr_3Si$ building blocks, and derives from this, with crystallographic shear operations (CS) in the (220) planes, a hypothetical

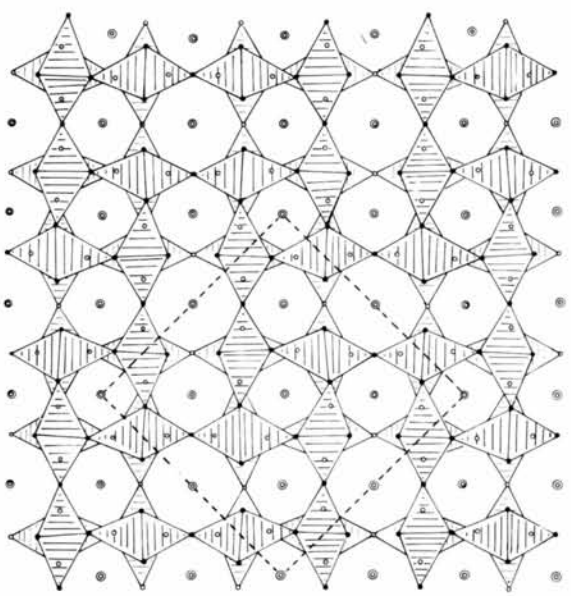

Fig. 1. Real structure of $Mo_3CoSi$ with tetragonal cell outlined. Square antiprisms at (0,0,1) and ($\frac{1}{2},\frac{1}{2},1$). Hexagonal antiprisms at ($\frac{1}{2}$,0,1).

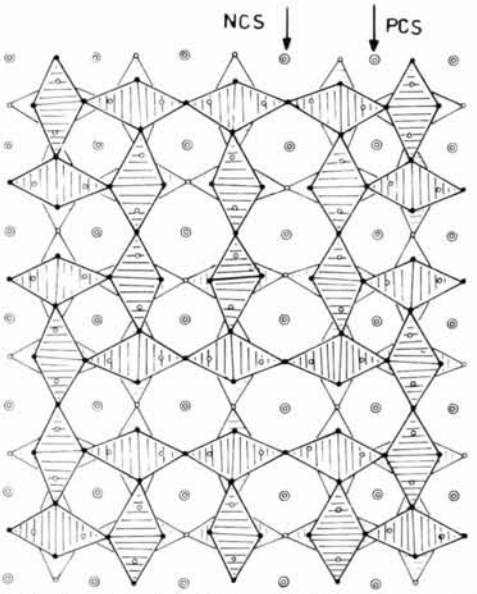


Fig. 2. The structure after NCS and PCS have been carried out.

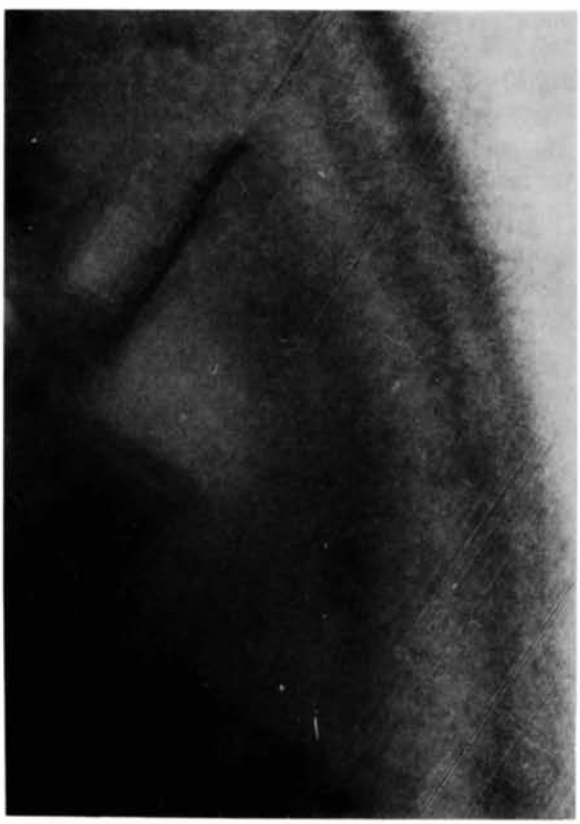

Fig. 3. Micrograph of a $Mo_3CoSi$ crystal at lower magnification.

structure with 2 × 1 $Cr_3Si$ blocks. This will hereafter be called positive CS (PCS). The opposite shear operation in the (110) plane of the $Mo_3CoSi$ structure results in negative CS (NCS), and will, if carried out in the (110) planes, give a structure of 2 × ∞ $Cr_3Si$ blocks.

It is of course possible to combine these two operations in different ways, giving structures of various block sizes. Fig. 2 shows the structure obtained if PCS and NCS are operated on the $Mo_3CoSi$ structure, resulting in blocks of 2 × 3.

Fig. 3 is a micrograph, at lower magnification, of a $Mo_3CoSi$ crystal, indicating the presence of different defects all over the crystal. Fig. 4 gives the corresponding diffraction pattern. In Fig. 5 a part of the same crystal is seen at higher magnification. The spacing between the bright dots is 8·94 Å in the ordered parts, corresponding to half the diagonal in the tetragonal cell. The bright spots arise from the hexagonal antiprisms, and the somewhat darker dots in between indicate the square antiprisms.

Calculated images, using the multislice method (Cowley & Moodie, 1957; Goodman & Moodie 1974), were computed with a program written by P. Fejes & J. Skarnulis at Arizona State University, USA. Fig. 6 shows a calculated image of $Mo_3CoSi$ with the ordering given by Gladyshevskii, Kripyakevich & Skolozdra (1967).

The bright dots visible in the defects in Fig. 5 lie approximately 5·0 × 8·9 Å apart. This agrees very well with the structure mentioned above, 2 × 3 $Cr_3Si$ blocks, and shown in Fig. 2. These defects run infinitely through the crystal, and cannot be terminated with the operations mentioned earlier. Identical shear operations in planes perpendicular to the first ones can be carried

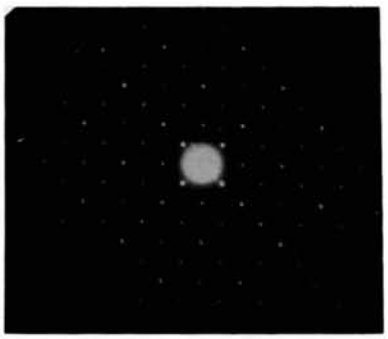

Fig. 4. Reciprocal lattice of the $Mo_3CoSi$ crystal. Strong reflexions along the diagonals.

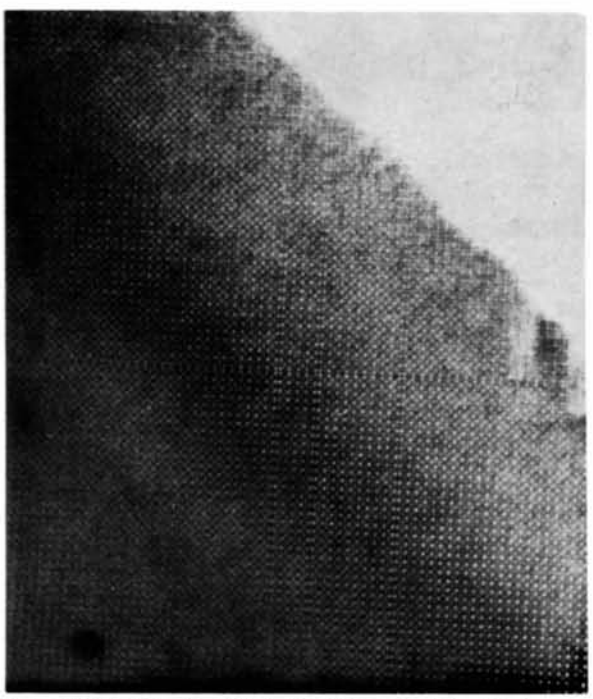

Fig. 5. Micrograph at higher magnification. Distance between bright dots is 8·94 Å in the ordered parts. The atomic arrangement for the single defects is drawn in Fig. 2, and for the crossing defects in Fig. 7. Defocus – 1000 Å.

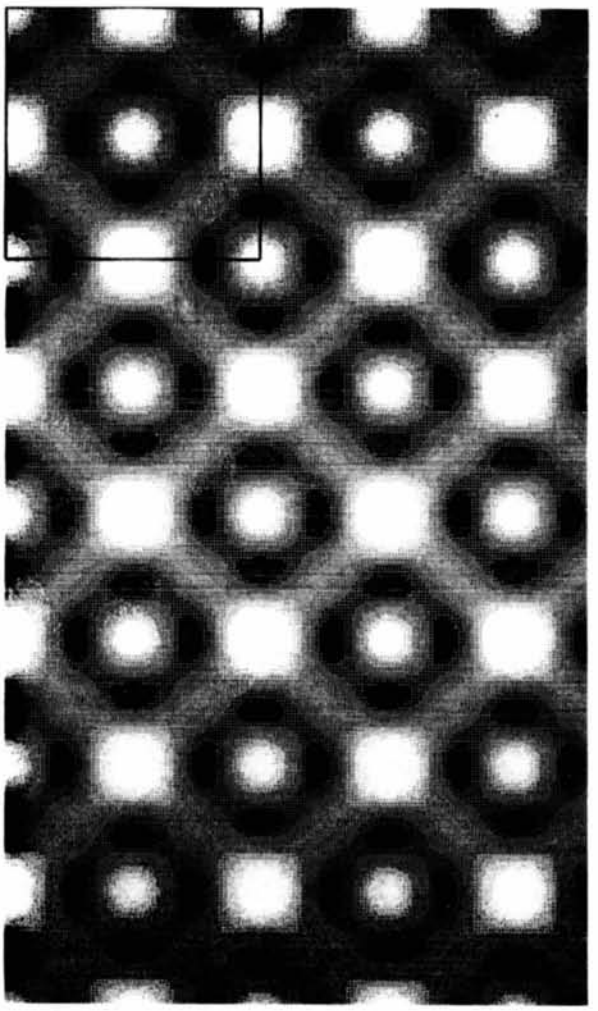

Fig. 6. Calculated image of $Mo_3CoSi$. Tetragonal axes outlined in upper left corner. Defocus – 1100 Å.

out. In the micrograph in Fig. 5 a square of bright dots is formed at the junction between two crossing shear-planes. This square, with an edge of 5 Å, is a piece of the $Cr_3Si$ structure, which can be seen in Fig. 7.

Fig. 8 shows three defects running parallel to each other, with one part of the original $Mo_3CoSi$ structure in between. This gives a bigger part of the earlier described 2 × 3 block structure, as shown in Fig. 9.

In various crystals of $Mo_3CoSi$ other kinds of defects were also observed to which detailed atomic arrangements could be given. These will be dealt with in a forthcoming article.

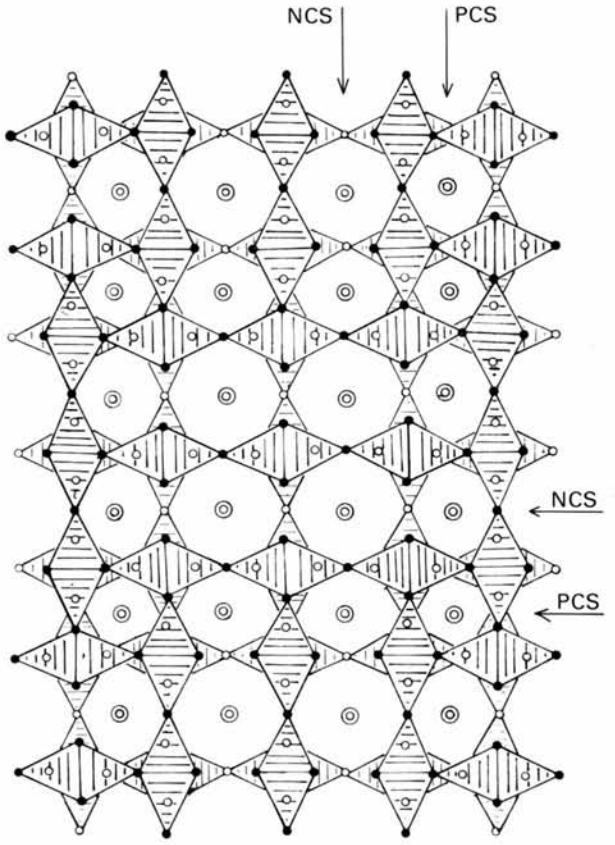


Fig. 7. The structure after NCS and PCS have been carried out in perpendicular planes. A 3 × 3 block structure will result if shear operations are carried out consequently.

Fig. 8. Three parallel defects, giving a new ordered alloy structure.

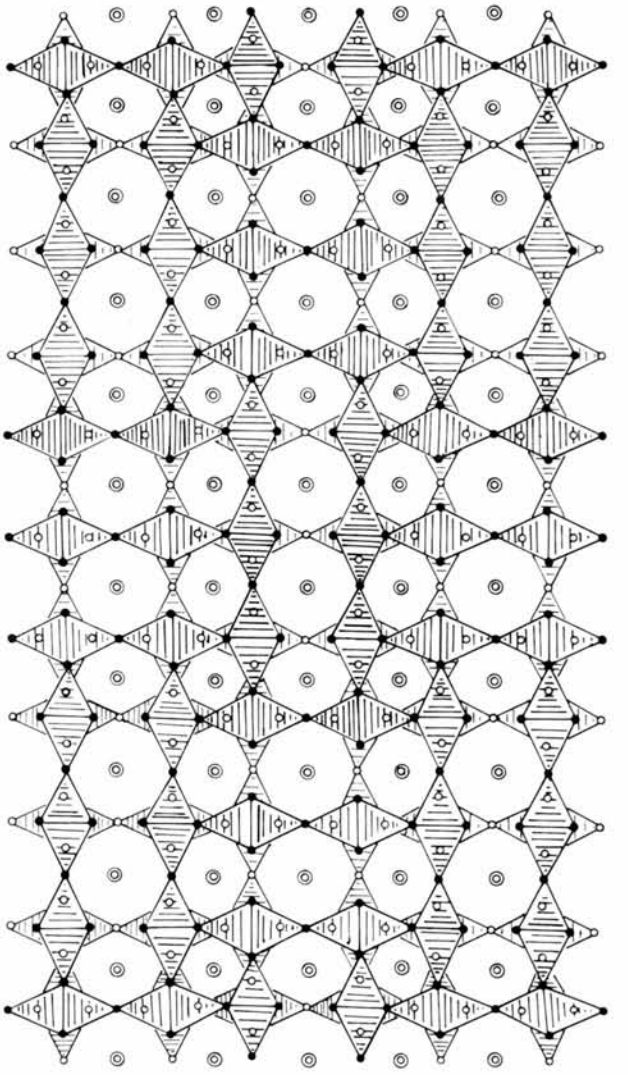

Fig. 9. Idealized structure of defect area in Fig. 8, giving a 2 × 3 block structure.

I wish to thank Dr Sten Andersson for valuable discussions.

This work was supported by the Swedish Natural Science Research Council.

### References

ANDERSSON, S. (1978). *J. Solid State Chem.* **23**, 191–204.

COWLEY, J. M. & MOODIE, A. F. (1957). *Acta Cryst.* **10**, 609–619.

GLADYSKEVSKII, E. J., KRIPYAKEVICH, P. I. & SKOLOZDRA, R. V. (1967). *Dokl. Akad. Nauk SSSR*, **175**, 1047–1050.

GOODMAN, P. & MOODIE, A. F. (1974). *Acta Cryst.* A**30**, 280–290.

STENBERG, L. & ANDERSSON, S. (1978). *J. Solid State Chem.* In the press.